Structure and properties of detonation coatings Al_2O_3 and $MgAl_2O_4$ on refractory materials for lining of steelmaking vessels

S. V. Zaitsev, *Research Engineer, Center of High Technologies* [1], *e-mail: sergey-za@mail.ru;*
V. V. Strokova, *Dr. Eng., Prof., Head of Dept. of Material Science and Materials Technology* [1], *e-mail: s-nsm@mail.ru;*
V. V. Sirota, *Cand. Phys.-Math.,Director of the Center of High Technologies* [1], *e-mail: zmas36@mail.ru;*
D. O. Bondarenko, *Cand. Eng., Associate Prof., Dept. of Material Science and Materials Technology* [1], *e-mail: di_bondarenko@mail.ru*

[1] *Belgorod State Technological University named after V. G. Shukhov (Belgorod, Russia)*

It is very important to provide output of high-quality metallurgical products with minimal production expenses. In this field, iron and steel production occupies about 70 % of total volume of manufactured refractories. In this case, equipping of steelmaking vessels with high-quality lining is considered as one of the key goals, while this lining ensures stable and safe iron and steel production even at the extra high temperatures. Alumosilicate refractories are widely used in the metallurgical industry; however, their operation in aggressive conditions is accompanied by corrosion and erosion, what decreases substantially the service life of high-temperature steelmaking vessels. To solve this problem, development of protective coatings, which are able to restrict interaction of operating media with material surface and to rise its corrosion resistance, is required. This research examines possibility of using the method of detonation spraying with applying of a multi-chamber cumulative-detonation unit for creation of protective coatings presented by aluminium oxide (Al_2O_3) and magnesium aluminate spinel ($MgAl_2O_4$) for alumosilicate refractories. The conducted investigations were aimed on evaluation of structure and properties of detonation coatings; they displayed that dense coatings of corundum and spinel with lamellar structure are forming on the surface of high-alumina refractories. Such coatings decrease refractory surface roughness by 45 % and are characterized by average thickness ~300 μm, porosity < 3.25 % and microhardness ~1300 HV_{03}. The results of this research confirm prospectivity of applying the detonation spraying technology for refractory materials as a possible method for lining protection of steelmaking vessels.

Key words: alumosilicate refractories, Al_2O_3 coatings, $MgAl_2O_4$ coatings, detonation spraying, structure, microhardness, lining, steelmaking vessels.
DOI: 10.17580/cisisr.2025.01.07

Introduction

About 70 % of all manufactured refractory materials are used in iron and steel production, where they play an important role, providing holding of metal melts, slags and gases [1]. Conventional alumosilicate refractories, characterizing by high melting temperature and resistance to extremal thermal loads, are widely used in various industrial branches, especially in ferrous metallurgy [2–4]. E.g., high-alumina refractories of the system Al_2O_3–SiO_2, which are manufactured via the ceramic technology, are actively used in steelmaking processes as special shape elements for steelmaking ladles. These elements include responsible components for metal guides, collector sleeves, stopper-rod devices etc., however, they are subjecting to intensive erosion under the effect of molten steel, what can provide negative effect on quality of finished products [5]. During recent years, especial attention in the process of high-quality steel production is paid to refractories, which were manufactured on the base of low-carbon corundum graphite (Al_2O_3–C) and low-carbon magnesial graphite composition (MgO–C) [6–10]. However, the materials on the base of magnesial aluminate spinel ($MgAl_2O_4$) and corundum (Al_2O_3) demonstrate essential advantages, including absence of carbon and silicon in their composition; it decreases risk of contamination of molten steel [11, 12]. Corundum is known for its high wear resistance and refractory resistance (the melting temperature in higher than 1790 °C), so it is often added in compositions on the base of magnesial aluminate spinel to be used in the processes of iron and steel melting [13–16]. Magnesial aluminate spinel, in its turn, is characterized by increased cracking resistance and resistance to slag erosion, what makes it especially valuable for protection of refractories in the conditions of aggressive high-temperature media [17–20].

Refractories are subjected to intensive degradation in the operating conditions due to corrosion and erosion, which are caused by the contact with molten steel and slags, as well as by thermal cracking owing to sudden temperature drops [21, 22]. It leads to decrease of lining service life, to increase of expenses for their replacement and maintenance of industrial units. The studies show that physical penetration of steel and slag melts in material pores are considered as the main causes of refractories destruction; it leads to corrosion and erosion wear. In this connection, increase of corrosion and erosion resistance of refractories, as well as prolongation of lining service life in high-temperature units is one of the key goals in iron and steel production. Use of expensive refractory compositions is not always justified economically, thereby applying the protective coating on the surface of alumosilicate refractories becomes an alternative technical solution. These coatings block penetration of aggressive substances and minimize direct contact between refractory material and steel, slags and gases, what ensures saving construction integrity in the extremal operating conditions.

This research is aimed on obtaining high-quality Al_2O_3 and $MgAl_2O_4$ coatings with minimal porosity in high-alumina refractory materials, using the method of detonation spraying, which was realized with applying of a multi-chamber cumulative-detonation unit. Especial attention is paid to parameters of obtained coatings, such as microhardness, porosity and structure, to establish their correlation with functional stability in the extremal conditions of blast furnace and steelmaking processes. The obtained data confirm prospectivity of introduction of these materials in metallurgical practice for increasing service life of refractory elements during the contact with iron and steel melts.

Materials description and analytical methods

To obtain ceramic coatings, alumina powder and the mixture of alumina and periclase powder (with relationship 71:29) were used as raw materials in correspondence with the work [23]. Mixing of alumina powder and periclase was carried out in a three-axial mixer C2.0 "TURBULA" during 60 min, with mass relation between balls and mixture 1:2 and speed 25 min^{-1}. Coatings application was conducted via the method of detonation spraying on refractory material using multi-chamber cumulative detonation unit (MCDU) technology [24] in correspondence with the parameters presented in the **Table 1**. High-alumina refractory bricks MKS-72 (fabricated according to the GOST 24704-94) were used as refractory material. Each brick was sheared for samples with size 50×50×7 mm and cleaned by compressed air under the pressure 2 MPa, achieving at least the first class of contamination according to the GOST 17433-80.

Crystallographic phases of initial powders and high-alumina refractory, as well as of coatings, were determined using Cu Kα radiation, via X-ray diffractometer ARL X'TRA ThermoTechno within the range 10–80° and via X-ray diffractometer ARL 9900 WorkStation, respectively. To decode diffraction patterns, the database of the International Center JCPDF for diffraction data was used. Distribution of sizes of particles was determined using laser analyzer of particles FRITSCH Analysette 22 NanoTec plus in correspondence with the GOST 8777-2011 [25].

Form of the particles, their cross sections, surfaces of both coatings and refractory were analyzed using scanning electron microscopy (SEM) TESCAN MIRA 3 LMU. Surface morphology and topography were analyzed via the software and hardware complex SIAMS-800 (Ekaterinburg). Coating porosity was determined via image analysis with use of software ImageJ in accordance to standard ASTM E2109-01 [26]. Porosity was evaluated as an average value of four dimensions in micro-pictures, which were occasionally captures on polished cross-sections of coated samples. The detailed procedure of porosity evaluation is described in the work [27]. Open porosity of high-alumina refractory was determined in accordance to the GOST 2409-2014. Cross-sections and surfaces of coatings, as well as refractories were ground and polished according to the standard ASTM E1920 [28] in order to obtain mean arithmetic roughness (R_a) less than 0.2 μm. Hardness of coatings was measured on polished surfaces by Vickers indentor under load 2.94 N (HV_{03}) using calibrated sensor Nexus 4000. Vickers hardness was measured by at least 10 acceptable prints, which were obtained via force applying during 15 s, without varying material hardness with applied load.

Discussion of results

Surface morphology and diffraction pattern of high-alumina refractory are shown in the **Fig. 1**. Surface analysis of high-alumina refractory (**Fig. 2**) displays presence of irregular grains with low sintering degree, what stipulates its low density (2.5 g/cm^3) and high open porosity (24 %); it is typical for pressing and sintering processes. Additionally, craters and macropores, which are located between grains, are observed on material surface. The mean arithmetic value of surface roughness R_a was equal to 42.7 μm. The diffraction pattern (see Fig. 2*b*) confirms presence of two main phases – mullite and corundum, what is typical for high-alumina refractories.

Microscopy and diffraction patterns of two powders (pure alumina and the mixture of alumina and periclase) are shown

Table 1. Conditions of coatings application

Parameters	Alumina powder	Alumina and periclase powder
Consumption of fuel mixture components: [m^3/h]		
– air	1.41*/0.85**	
– oxygen	3.13*/3.68**	
– propane/butane (40/60 %)	0.63*/0.68**	
Transporting gas – air	0.9	
Powder feed [g/h]	110	150
Spraying distance [mm]	50	
Channel length [mm]	500	
Internal nozzle diameter [mm]	16	
Motion speed along the sample [mm/min]	2000	
Number of spraying passes	16	16

* – cylinder chamber of combustion, ** – circular chamber of combustion

in the Fig. 2. Microscopy of these powders demonstrates differences in surface morphology of alumina and the mixture of powders after mechanical mixing.

The typical alumina structure, containing of the particles with micrometer dimensions with separate spherical particles, can be seen in the Fig. 2*a*; it is typical for the powders fabricated via agglomeration and sintering processes. Fig. 2*b* presents microstructure of the mixture, which was obtained via mixing of alumina and periclase (with mass relationship 71:29) in a three-axial mixer. The process of mechanical mixing leads to partial variation of initial powder morphology owing to intensive interaction of the particles among themselves and with balls, what provides more homogeneous distribution of phases and partial refining and deformation of the particles; it is observed in the form of more complicated aggregate structure.

Analysis of granulometric composition of alumina powder particles and its mixture with periclase revealed the following parameters of distribution according to the sizes. The values for alumina, which determine the boundaries with location of 10 %, 50 % and 90 % of volume of particles below them are d10 = 2.28 μm, d50 = 19.96 μm and d90 = 46.36 μm. For the mixture of alumina and periclase, these parameters were equal to d10 = 3.77 μm, d50 = 23.52 μm and d90 = 49.83 μm.

The typical peak maximal values, corresponding to the crystalline structure of pure alumina with the phase γ—Al_2O_3

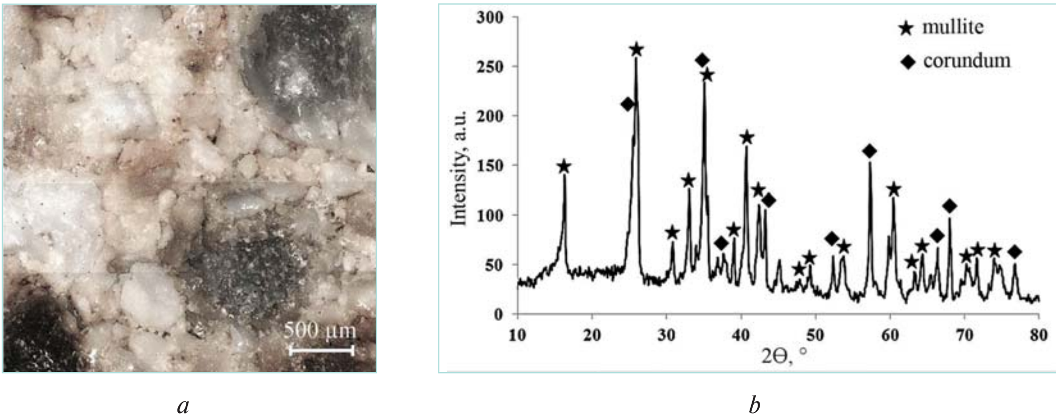

Fig. 1. Surface morphology (*a*) and diffraction pattern (*b*) of high-alumina refractory

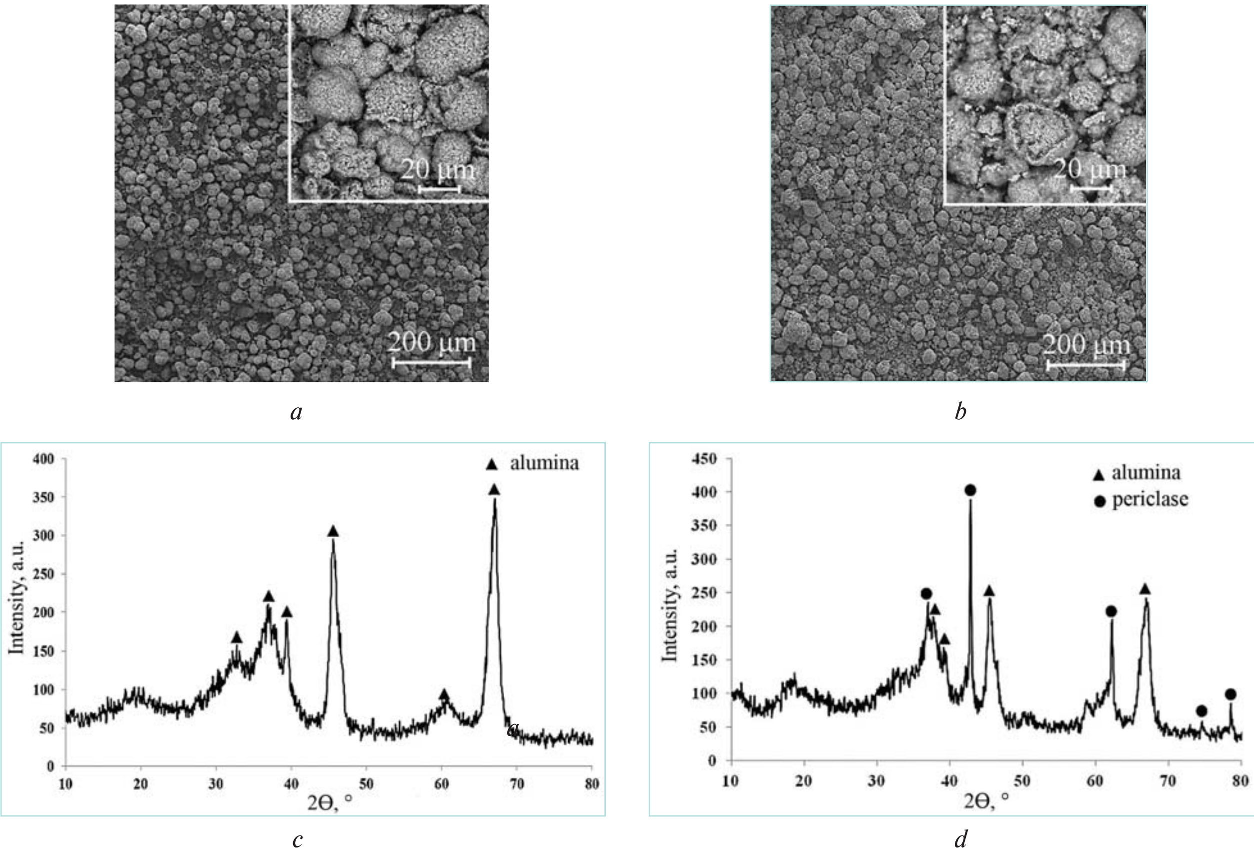

Fig. 2. Morphology (*a, b*) and diffraction pattern (*c, d*) of alumina powders (*a, c*) and the mixture of alumina and periclase (*b, d*)

(ICDD/JCPDS No. 10-425) is seen in the diffraction pattern of alumina powder (Fig. 2*c*). The diffraction pattern of the mixture of powders (Fig. 2*b*) demonstrates additional peaks, which show presence of periclase in the mixture; each of the components saves its diffraction parameters, what allows to characterize both alumina and periclase in the mixture composition. Respectively, $\gamma{-}Al_2O_3$ (ICDD/JCPDS No. 10-425) and MgO (ICDD/JCPDS No. 45-946) are classified as crystalline phases.

Diffraction patterns of the coatings are displayed in the **Fig. 3**. Analysis of this diffraction pattern, which was obtained during alumina detonation spraying (Fig. 3*a*), shows, that the main part of peaks corresponds to the phase $\alpha{-}Al_2O_3$, and also the peaks typical for the phase $\gamma{-}Al_2O_3$, are noted. It testifies that the technology of detonation spraying causes substantial variations in the material crystal lattice, ensuring transition from γ-phase to more stable α-phase. Presence of the small part of the phase $\gamma{-}Al_2O_3$ is explained by the observation that the particles have no time to be molten completely during striking at the substrate surface of a sample, due to high cooling speed. It is connected with smaller amount of intra-phase energy of the phase $\gamma{-}Al_2O_3$ in comparison with the phase $\alpha{-}Al_2O_3$, what hinders finalizing of phase transformation in the conditions of quick cooling [29–31]. It should be noted that the molten particles, which were subjected to intensive heating during spraying process, can be characterized by different through heating at the moment of striking the substrate. It depends both on their sized and flow speed of powder particles. As a result, the particles with more long temperature holding period (about 1100 °C) have more chances to transfer in a metastable α-phase, what is just observed in the examined coating.

The applied coating of the mixture of alumina and periclase is characterized by high content of crystalline magnesium aluminate spinel ($MgAl_2O_4$) (Fig. 3*b*) and also by presence of the secondary periclase phase (MgO). Probably, forming of the secondary periclase phase is connected with excessive MgO content in the initial powder. Presence of the corundum phase ($\alpha{-}Al_2O_3$) was not revealed, what testifies on complete $\gamma{-}Al_2O_3$ consumption for forming of the spinel phase. These data confirm that magnesium aluminate spinel coating is forming as a result of solid phase diffusion reaction between MgO and $\gamma{-}Al_2O_3$ during the process of detonation spraying.

No delaminating or exfoliation of coatings was revealed during visual analysis of the surface of samples using optical microscope (**Fig. 4**). Use of the detonation method of spraying on refractory material provides high homogeneity of material distribution along the surface. The coatings, which were applied both by pure alumina and the mixture of alumina and periclase, are characterized by smooth texture with roughness parameters R_a = 25.9 µm and R_a = 23.3 µm respectively, in comparison with the surface of high-alumina

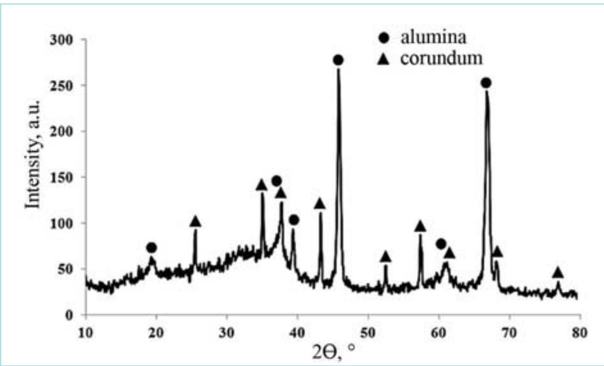

a

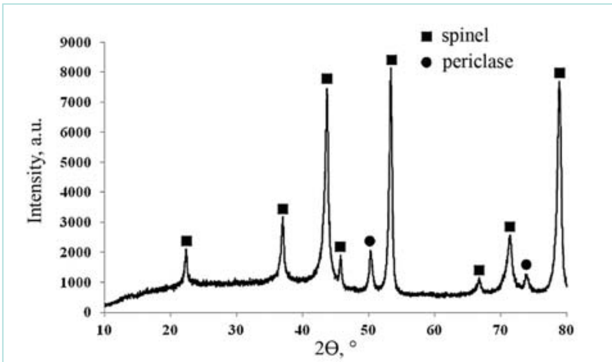

b

Fig. 3. Diffraction pattern of coatings of alumina powder (*a*) and the mixture of alumina and periclase (*b*), applied on the samples

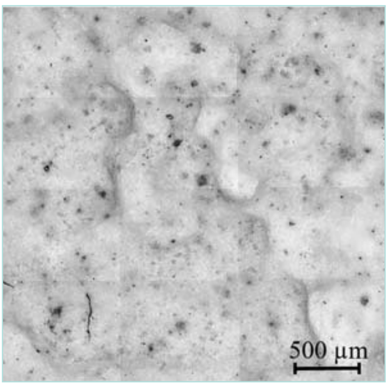

a

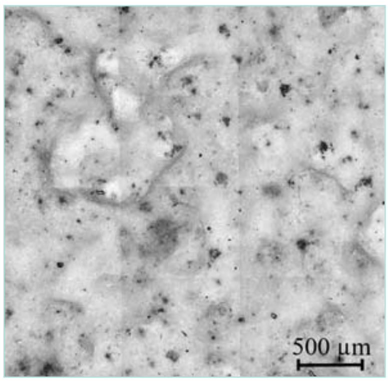

b

Fig. 4. Morphology of the surface of coatings Al_2O_3 (*a*) and $MgAl_2O_4$ (*b*), obtained using optical microscope

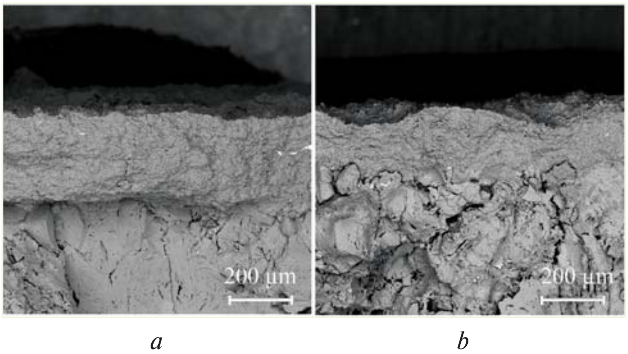

Fig. 5. Cross-section of refractory with aluminium oxide (*a*) and spinel (*b*) coatings

refractory with $R_a = 42.7$ µm. Additionally, all pores and craters among the particles were filled completely, what means high quality of the obtained coatings.

Study of microstructure of the coatings (**Fig. 5**), which were carried out using SEM, displayed that average thickness of Al_2O_3 and $MgAl_2O_4$ coatings was about 305 µm and 252 µm respectively. These coatings are characterized by lamellar structure without visible defects, such as microcracks and pores. Forming of lamellar structure occurs due to the strong effect of powder particles on the surface of alumosilicate refractory. A powder particle strikes to the surface and forms spot-shaped morphology, while such consequent actions lead to forming of lamellar structure, which is observed in the most part of thermally sprayed coatings. This process takes place in parallel direction to the surface and such structure becomes possible when powder particles strike to the surface with high speed. No gap between the coating and alumosilicate refractory is observed, what manifests about strong physical link. Good adhesion can be explained by strong effect of the particles on the surface of alumosilicate refractory, what not only allows accurate spreading of drops with forming of spots, but also ensures the tendency of well adhesion between drops and refractory surface, owing to their molten state. It also promotes good connection between plates, what significantly restricts forming of defects.

Thus, the coating not only forms the reliable protective layer on the surface of high-alumina refractory, but also compensates its structural disadvantages via filling cracks and pores. It improves substantially its protective properties, increasing its corrosion resistance in silicate melts.

The results of measuring porosity and hardness of the coatings are shown in the **Fig. 6**. It can be seen that corundum coating is characterized by porosity 2.04 %, while spinel coating has porosity 3.25 % (Fig. 6*a*). These indicators are rather lower in comparison with porosity level for high-alumina refractory, which makes 24 %; it can be explained by more dense structure of coatings.

According to the results of microhardness measurements (Fig. 6*b*), which were conducted with use of Vickers hardness meter, the maximal hardness of the coating applied from alumina powder and from the mixture of powders achieves 1336 HV_{03} and 1277 HV_{03} respectively. It should be noted at the same time, that it is difficult to provide measuring the refractory surface hardness owing to heterogeneity of its structure (including corundum and mullite grains [32]) as well as presence of glass phase in its structure. As it was mentioned above, high-alumina refractory is characterized by low degree of sintering ability, what makes more complicated obtaining of the exact data. Based on this, the average hardness of refractory is lower in comparison with hardness of refractory with coating.

Conclusion

Ceramic coatings of corundum (Al_2O_3) and magnesium aluminate spinel ($MgAl_2O_4$), which were applied by the method of detonation spraying with use of a multi-chamber cumulative-detonation unit, were successfully applied on the surface of high-alumina refractory materials. It was established that phase variations of initial powders with forming of new phases are observed in the applied coatings on the base of alumina powder and from the mixture of alumina and periclase. Domination of the $\alpha{-}Al_2O_3$ phase with slight content of the $\gamma{-}Al_2O_3$ phase is typical for pure alumina with the $\gamma{-}Al_2O_3$ phase, while for the mixture of alumina and periclase, forming of magnesium aluminate spinel ($MgAl_2O_4$) with slight periclase content is noted.

Microstructural analysis displayed that use of the technology of detonation spraying allows obtaining of high-homogeneous coatings, which completely fill pores and craters on the surface of refractory material. It leads to substantial reducing of mean square roughness of the surface from

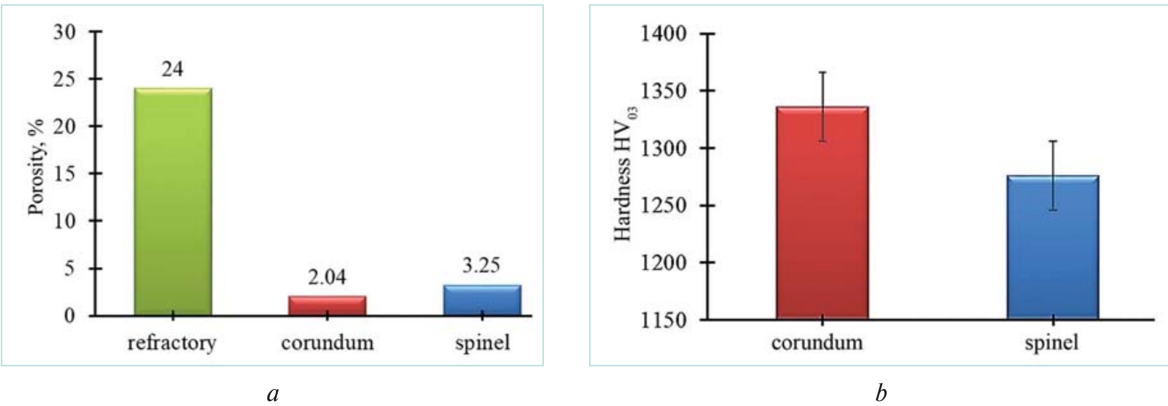

Fig. 6. Porosity (*a*) microhardness (*b*) of the coatings

initial 42.7 μm to 25.9 μm and 23.3 μm, for corundum and spinel coatings respectively. Forming of the typical lamellar structure of coatings without visible defects (such as cracks and pores) is observed; it provides reliable physical adhesion with high-alumina refractory and promotes minimizing of defect forming during operation. It was established that the obtained coatings are characterized by low porosity: 2.04 % for Al_2O_3 and 3.25 % for $MgAl_2O_4$ in comparison with porosity level for high-alumina refractory, which makes 24 %; it improves essentially protective properties of refractories. Comparative analysis of microhardness displayed the high hardness values both for corundum (1336 HV_{03}) and spinel (1277 HV_{03}) coatings, what confirms their high wear resistance.

Based on the obtained results, it can be concluded that detonation coatings on the base of Al_2O_3 and $MgAl_2O_4$ can be recommended as protective layers on refractory materials in high-temperature steelmaking vessels. Further investigations will be directed on evaluation of corrosion resistance of refractories with detonation coatings in real operating conditions.

The research was carried out within the framework of realization of the state assignment of the Ministry of Science and Education and Science of Russian Federation No. FZWN-2023-0006 with use of equipment of the Center of high technologies in the Belgorod State Technological University named after V. G. Shukhov

REFERENCES

1. Kerber F., Zienert T., Neumann M., Malczyk P., Schemmel T., Jansen H., Aneziris C. G. Insulating refractories based on rice husk ashes functionalized by flame-sprayed alumina coatings for steel ingot casting. *Journal of the European Ceramic Society*. 2024. Vol. 44. No. 12. pp. 7296–7309.
2. Pletnev P. M., Pogrebenkov V. M., Vereshchagin V. I., Tyulkin, D. S. Mullite-corundum materials based on mullite binder resistant to high-temperature deformation. *Refractories and Industrial Ceramics*. 2018. Vol. 58. No. 6. pp. 618–625.
3. Soltan A. M., Pöllmann H., Kaden R., König A., Abd El-Raoof F., Eltaher M., Serry M. Degradation of aluminosilicate refractories: An integrated approach. *Journal of the European Ceramic Society*. 2015. Vol. 35. No. 16. pp. 4573–4592.
4. Khanmohammadi S., Mohtadinia M. High temperature corrosion resistance of various aluminosilicate refractory bricks. *Ceramics International*. 2024. Vol. 50. No. 23. pp. 49125–49133.
5. Wang Y., Zhang J., Wang C., He D., Qin H., Li H. The corrosion behavior of Al_2O_3–SiO_2 refractory in reducing atmosphere. *Ceramics International*. 2024. Vol. 50. No. 23. pp. 51550–51559.
6. Myung J., Chung Y. Degradation Behavior of MgO–C in Contact With Liquid Steel Without/With Ar Blowing. *Metallurgical and Materials Transactions B*. 2024. Vol. 55. No. 1. pp. 83–91.
7. Hwang I., Chung Y. Physical and Chemical Wetting Behavior Between MgO–C and Liquid Slag With Varying Slag Composition. *Metallurgical and Materials Transactions B*. 2023. Vol. 54. No. 6. pp. 2881–2888.
8. Chen Y., Li Z. Y., Tan H. B., Fu Y. R., Ding J., Deng C. J.,Yu C. Effect of micro-Al_2O_3 powders on oxidation and corrosion behaviors of low-carbon MgO–C refractories. *Journal of Iron and Steel Research International*. 2024. Vol. 31. No. 6. pp. 1522–1534.
9. Wu Z., Chen J., Miao Z., Yan J., Liu C., Yan W., Li N. Brittleness reduction of Al_2O_3–C refractories: Microstructure evolution and role of carbon fibers. *Ceramics International*. 2024. Vol. 50. No. 18. pp. 32163–32170.
10. Zhang T., Chen T., Liu Z., Yu C., Deng C., Ding J., Cheng C. Enhancement and evaluation of strength stability of low-carbon Al_2O_3–C refractories based on ceramic phase distribution modulation. *Ceramics International*. 2025. Vol. 51. No. 4. pp. 4946–4956.
11. Ma B., Yin Y., Zhu Q., Zhai Y., Li Y., Li G., Yu J. Slag corrosion and penetration behaviors of $MgAl_2O_4$ and Al_2O_3 based refractories. *Refractories and Industrial Ceramics*. 2016. Vol. 56. pp. 494–501.
12. Zhang W. W., Zheng W., Yan W., Li G. Q. Formation mechanism of interface reaction layer between microporous magnesia refractories and molten steel and its effect on steel cleanliness. *Journal of Iron and Steel Research International*. 2023. Vol. 30. No. 9. pp. 1743–1754.
13. Zhao P., Zhang H., Gao H., Zhu Y., Yu J., Chen Q., Zhao H. Separation and characterisation of fused alumina obtained from aluminium-chromium slag. *Ceramics International*. 2018. Vol. 44. No. 4. pp. 3590–3595.
14. Hossain S. S., Roy P. K. Preparation of multi-layered (dense-porous) lightweight magnesium-aluminum spinel refractory. *Ceramics International*. 2021. Vol. 47. No. 9. pp. 13216–13220.
15. Huang A., Wang Y., Gu H., Zou Y. Dynamic interaction of refractory and molten steel: effect of alumina-magnesia castables on alloy steel cleanness. *Ceramics International*. 2018. Vol. 44. No. 18. pp. 22146–22153.
16. Abyzov A. M. Aluminum oxide and alumina ceramics (review). Part 1. Properties of Al_2O_3 and commercial production of dispersed Al_2O_3. *Refractories and industrial ceramics*. 2019. Vol. 60. pp. 24–32.
17. Angappan S., Berchmans L. J., Augustin C. O. Sintering behaviour of $MgAl_2O_4$ a prospective anode material. *Materials Letters*. 2004. Vol. 58. No. 17–18. pp. 2283–2289.
18. Bocanegra S. A., Ballarini A. D., Scelza O. A., de Miguel S. R. The influence of the synthesis routes of $MgAl_2O_4$ on its properties and behavior as support of dehydrogenation catalysts. *Materials chemistry and physics*. 2008. Vol. 111. No. 2–3. pp. 534–541.
19. Chen Z., Yan W., Schafföner S., Zhi J., Li N. Vacuum impregnation treatment of microporous Al_2O_3–$MgAl_2O_4$ refractory raw materials with sub-micron pores and high strength. *Journal of the European Ceramic Society*. 2022. Vol. 42. No. 12. pp. 5145–5152.
20. Tadić A. P., Živojinović J., Pavlović V., Stanković A., Filipović S., Obradović N., Kern F. The influence of mechanical activation and sintering process on the formation of the spinel phase of $MgAl_2O_4$. *Journal of the Australian Ceramic Society*. 2025. pp. 1–7. doi.org/10.1007/s41779-024-01144-1
21. Sidorina E. A., Isagulov A. Z., Kashcheev I. D., Zemlyanoi K. G. Production and Development of Superdense Slag-Resistant Aluminosilicate Refractories. *Refractories and Industrial Ceramics*. 2022. Vol. 63. No. 3. pp. 280–282.
22. Mulevanov S. V., Nartsev V. M., Doroganov V. A., Doroganov E. A., Zaitsev S. V. Aspects of the corrosion of refractories in structured aggressive media. *Refractories and Industrial Ceramics*. 2012. Vol. 53. No. 4. pp. 226–2228
23. Szczerba J., Pędzich Z., Nikiel M., Kapuścińska D. Influence of raw materials morphology on properties of magnesia-spinel refractories. *Journal of the European Ceramic Society*. 2007. Vol. 27. No. 2–3. pp. 1683–1689.
24. Kolisnichenko O. V., Tyurin Yu. N., Tovbin R. Efficiency of process of coating spraying using multichamber detonation unit. *The Paton welding journal*. 2017. No. 10. pp. 18–23.
25. GOST 8.777-2011. Dispersed composition of aerosols and suspensions. Determination of sizes of particles via diffraction of laser radiation.
26. ASTM E2109-01.-2014. Standard Test Methods for Determining Area Percentage Porosity in Thermal Sprayed Coatings.
27. Du H., Lee S.W., Shin J.H. Study on porosity of plasma-sprayed coatings by digital image analysis method. *Journal of thermal spray technology*. 2005. Vol. 14. pp. 453–461.
28. ASTM E1920-03.-2021. Standard Guide for Metallographic Preparation of Thermal Sprayed Coatings.
29. Damani R.J., Makroczy P. Heat treatment induced phase and microstructural development in bulk plasma sprayed alumina. *Journal of the European Ceramic Society*. 2000. Vol. 20. No. 7. pp. 867–888.
30. Yin Z., Tao S., Zhou X., Ding C. Particle in-flight behavior and its influence on the microstructure and mechanical properties of plasma-sprayed Al_2O_3 coatings. *Journal of the European Ceramic Society*. 2008. Vol. 28. No. 6. pp. 1143–1148.
31. Sirota V. V., Zaitsev S. V., Limarenko M. V., Prokhorenkov D. S., Churikov A. S. Effect of powder morphology on the structure and properties of Al_2O_3 based coatings obtained by detonation spraying. *Construction Materials and Products*. 2024. Vol. 7. No. 5. pp. 1–10.
32. Raghdi A., Heraiz M., Sahnoune F., Saheb N. Mullite-zirconia composites prepared from halloysite reaction sintered with boehmite and zirconia. *Applied Clay Science*. 2017. Vol. 146. pp. 70–80.